Research in Pharmaceutical Sciences, February 2025; 20(1): 109-120
Received: 20-10-2023
Peer Reviewed: 25-02-2024
Revised: 11-03-2024
Accepted: 02-06-2024
Published: 20-02-2025

School of Pharmacy & Pharmaceutical Sciences
Isfahan University of Medical Sciences

Original Article

The development of mitochondria-targeted quercetin for rescuing Sertoli cells from oxidative stress

Satrialdi*, Cellina Pratiwi, Ryan Novia Khaeranny, and Diky Mudhakir*

Department of Pharmaceutics, School of Pharmacy, Institut Teknologi Bandung, Indonesia.

Abstract

Background and purpose: The imbalance between reactive oxygen species (ROS) production and endogenous antioxidant capacity leads to oxidative stress, which may damage several cellular functions, particularly spermatogenesis. This condition is a leading cause of male infertility, so controlling ROS levels is crucial. The ROS level can be controlled by supporting the endogenous antioxidant system through antioxidant therapy. Mitochondria are the prime target for antioxidant therapy due to the majority of endogenous ROS produced in mitochondria and their critical role in providing energy during fertilization. This research aimed to develop mitochondria-targeted hybrid nanoplatforms by combining liposomes with dequalinium's mitochondriotropic agent (DQ) to deliver quercetin for targeted antioxidant therapy to mitochondria.
Experimental approach: The quercetin-loaded nanocarrier was constructed using the hydration method. We varied the concentration of DQ to investigate its impact on physical characteristics, encapsulation efficiency, intracellular trafficking, and *in vitro* antioxidant activity.
Findings/Results: The impact of different DQ densities on particle size, encapsulation efficiency, and mitochondria targeting was insignificant. However, lowering the DQ density reduced the zeta potential. Minimizing oxidative stress on TM4 cells was only achieved with low-density DQ (Q-LipoDQ LD), while high-density DQ (Q-LipoDQ HD) failed to mitigate the negative impact.
Conclusion and implications: According to the findings, LipoDQ LD preserves a promising potential as mitochondria-targeted nanoplatforms and validates the importance of mitochondria as a target for antioxidant therapy.

Keywords: Antioxidant; Mitochondria-targeted drug delivery system; Therapy; Sertoli cells.

INTRODUCTION

Infertility is a public health problem that has a significant psychological impact on patients and their partners. According to the International Committee for Monitoring Assisted Technology (ICMART) and The World Health Organization (WHO), infertility is characterized as a disease of the reproductive system in which there is a failure to obtain pregnancy after 12 months or more of regular unprotected sexual intercourse. In this condition, reactive oxygen species (ROS) production exceeds the neutralizing capacity of endogenous antioxidants. Excessive production of ROS may lead to sperm membrane damage and reduction in sperm motility as well as loss of fusion ability with oocyte (1). Spermatozoa are very vulnerable to the harmful effects of ROS. This vulnerability is due to the plasma membrane and cytoplasm of spermatozoa containing polyunsaturated fatty acids in dominant amounts (2), where polyunsaturated fatty acid is a component that is very susceptible to the lipid peroxidation process induced by the presence of ROS (3,4).

*Corresponding authors:
Satrialdi, Tel: +62-222514316, Fax: +62-222504852
Email: satrialdi@itb.ac.id
D. Mudhakir, Tel: +62-222514316, Fax: +62-222504852
Email: mudhakir@itb.ac.id

Access this article online

Website: http://rps.mui.ac.ir

DOI: 10.4103/RPS.RPS_226_23

Furthermore, spermatozoa inherently possess limited deoxyribonucleic acid (DNA) repair mechanisms and contain small amounts of cytoplasmic antioxidants (5,6), rendering them more susceptible to elevated levels of ROS.

ROS is a unique molecule naturally produced as a by-product of metabolism, particularly during the mitochondrial electron transport chain (ETC). Some of the electrons may escape from the ETC and react spontaneously with oxygen molecules to form superoxide, which is rapidly neutralized by superoxide dismutase into another type of ROS, namely hydrogen peroxide (H_2O_2) (7). At low concentrations, ROS has an essential role in intracellular signaling, which can regulate several biological and physiological processes in the body (8), including spermatogenesis (9). Due to the high reactivity properties of ROS, they may damage several essential biomolecules, including protein, lipid, and nucleic acid. The uncontrolled ROS production may affect spermatozoa generation quantitatively and qualitatively (10). Therefore, controlling the concentration of ROS at a safe level is an essential effort to protect the function and process of spermatogenesis.

One of the main hotspots regarding the production of ROS inside the cells is mitochondria. Naturally, mitochondria produce ROS during their activities in synthesizing adenosine triphosphate (ATP) as the energy currency of cells. In the context of spermatogenesis and fertilization, mitochondria play crucial roles in providing energy and controlling the apoptosis process (11). Recent research reported that the depletion of mitofusins, proteins located in the outer mitochondrial membrane that control mitochondrial dynamics, hinders spermatogenesis (12). Thus, preserving mitochondrial function is crucial to support all processes related to male fertility. The control of mitochondrial functions can be achieved by delivering functional biomolecules such as antioxidants, proteins, and genetic materials into the mitochondria.

The transport of both small and large molecules into mitochondria is tightly regulated to preserve the critical functions of mitochondria. This condition leads to the requirement for a specific drug delivery system that can transport the functional biomolecules into the mitochondrial compartment of the cells (13). Moreover, solubility and stability issues are still a hurdle in achieving optimal therapeutic goals in antioxidant therapy. Several strategies have been developed to deliver antioxidants into mitochondria, including the use of delocalized lipophilic cations (14,15) such as triphenylphosphonium and dequalinium (DQ), peptide-based delivery (16), and nanocarrier system (17). However, a concern arises regarding the safety issue of drug delivery systems on mitochondrial function, such as using triphenylphosphonium, which has been reported to induce cytotoxicity through inhibition of the mitochondrial ETC (18). Therefore, developing a safe mitochondria-targeted drug delivery system is required.

As a first-generation mitochondriotropic, DQ has been extensively developed for mitochondria-targeted drug delivery. This compound can spontaneously form liposome-like structures in the aqueous phase, namely DQAsome (19). Due to its surface charge property, the DQAsome can interact electrostatically with the negatively charged mitochondrial membrane (20). However, the DQAsome has poor physical stability accompanied by low effectiveness of mitochondrial delivery and can induce mitochondrial dysfunction through the membrane potential depolarization process (21). One promising strategy to optimize DQ's benefits in targeting mitochondria could be the hybridization of DQ with other nanocarrier systems. Due to the amphiphilic characteristics of DQ, there is a potential to embed the DQ molecule inside the lipid bilayer structure of liposomes through hydrophobic interaction. By employing such a hybridization process, the concentration of DQ can be significantly reduced; thus, the direct negative effect on the mitochondrial membrane can be minimized while the mitochondria targeting ability is still maintained.

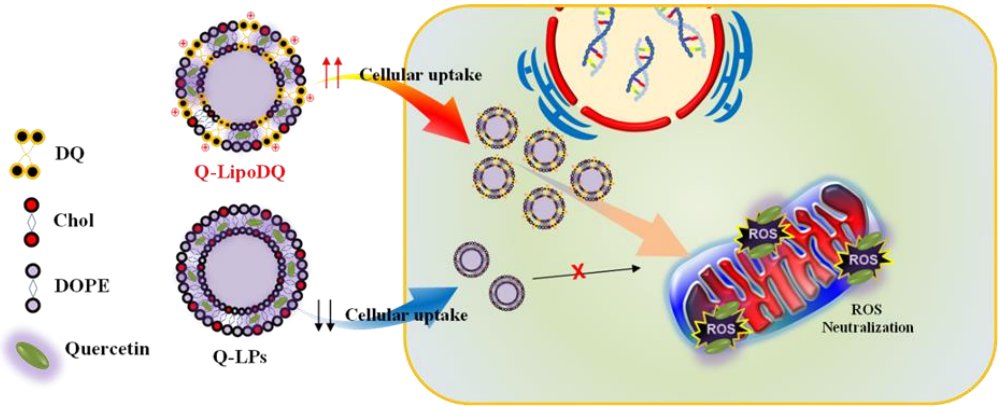

Fig. 1. Schematic illustration of the insertion of DQ into a liposomal structure consisting of DOPE and cholesterol with a molar ratio of 9:2. The presence of DQ moieties on the surface of Q-LipoDQ facilitates the mitochondrial accumulation of quercetin to proceed with effective ROS neutralization reaction. Q, Quercetin; LPs, liposomes; LD, low density; HD, high density; DQ, dequalinium; DOPE, 1,2-dioleyl-sn-glycero-3-phosphoethanolamine; ROS, Reactive oxygen species.

In the present study, we attempted to develop a mitochondria-targeted hybrid nanoplatform by inserting a mitochondriotropic agent of DQ into a liposomal nanostructure, namely LipoDQ. This nanocarrier system was employed to transport quercetin specifically into the mitochondria compartment of Sertoli cells, a group of cells that play an essential role in spermatogenesis, as they are the key component of the seminiferous tubule that provides nourishment for the development of spermatozoa. We evaluated the effect of DQ density on several properties, including physical characteristics, encapsulation efficiency (EE), intracellular trafficking, and *in vitro* antioxidant activity in Sertoli cells. The presence of DQ moieties on the surface of LipoDQ may enhance the cellular uptake efficiency and mitochondrial accumulation level by electrostatic interaction with negatively-charged membrane cells and mitochondria membranes, respectively. Furthermore, utilization of the fusogenic lipid of 1,2-dioleyl-*sn*-glycero-3-phospho-ethanolamine (DOPE) could further improve the endosomal escape ability. Finally, the specific mitochondrial delivery of quercetin, as a model antioxidant drug, can be involved in ROS neutralization, thus preventing the damaging effect of oxidative stress (Fig. 1).

MATERIALS AND METHODS

Materials

The materials used for preparing the liposomes and LipoDQ comprising DOPE, cholesterol, dequalinium chloride, and quercetin were purchased from Sigma Aldrich (St. Louis, MO, USA). The solvents, including methanol and ethanol, were obtained from Merck (Rahway, NJ, USA), while dimethyl sulfoxide (DMSO) was acquired from Sigma Aldrich (St. Louis, MO, USA). Dulbecco's modified eagle medium (DMEM), penicillin-streptomycin, fetal bovine serum (FBS), 3-(4,5-Dimethylthiazol-2-yl)-2,5-diphenyltetrazolium bromide (MTT reagent), and phosphate-buffered saline (PBS) were purchased from Thermo Fisher Scientific Inc. (Waltham, MA, USA). Mitotracker deep red FM and Hoechst 33342 were obtained from Invitrogen (Carlsbad, CA, USA). TM4 cells, mouse Sertoli cells, were obtained from the European Collection of Authenticated Cell Cultures (ECACC catalog number 88111401). All additional chemicals and solvents used were purchased as commercially available reagent-grade products.

Nanoparticle preparation

Quercetin-loaded LipoDQ (Q-LipoDQ) was constructed using the hydration method with the composition shown in Table 1. Briefly, the lipid films were prepared by mixing the ethanolic lipid solution of DOPE and cholesterol with 0.275 mM of methanolic quercetin solution and different concentrations of DQ in methanol solution (Table 1) followed by solvent evaporation using nitrogen gas. The resulting lipid films were hydrated using 10 mM of HEPES solution supplemented with 290 mM of glucose (pH 7.4) for 15 min at room temperature. The hydrated lipid films were

sonicated using a bath-type sonicator for 5 min to form a homogenous liposomal structure. To remove the non-encapsulated quercetin, the colloidal suspension was centrifuged at 16,000 rpm, 4 °C for 10 min. The supernatant was collected. To obtain a low density of Q-LipoDQ (Q-LipoDQ LD) and a high density of Q-LipoDQ (Q-LipoDQ HD) various concentrations of DQ were prepared. The non-mitochondria-targeted liposomes (Q-LPs) were also constructed using a similar method described above, which excluded the DQ solution from the formulation. Additionally, the mitochondrial accumulation level of the nanoparticles was analyzed through the constructed coumarin 6-labeled quercetin-loaded nanocarriers. We mixed the organic solvent containing the fluorescent dye of coumarin 6 with other components of nanocarriers before the solvent evaporation process. The concentration of coumarin 6 was set at 1/100 of the total lipid concentration.

Physical characterization of nanoparticles

The physical characteristics of all quercetin-loaded nanocarrier formulations were evaluated by determining the hydrodynamic diameter, particle size distribution, and zeta potential. The particle size and distribution were determined using the dynamic light scattering (DLS) method (Delsa Nano Particle Size Analyser and Zetasizer, Beckman Coulter, Brea, CA, USA). The zeta potential was evaluated using the laser Doppler electrophoresis method (Horiba, Montpellier, France).

Determination of quercetin EE and drug loading capacity

The concentration of quercetin encapsulated inside the nanoparticles was determined using the procedure reported by Chang *et al*. (22) with a minor modification. Briefly, the supernatant obtained from the centrifugation process was freeze-dried. The obtained powder was dissolved in methanol, and then $AlCl_3$ reagent and sodium acetate were added. The mixture was incubated for 30 min in dark conditions. The absorbance of the samples was measured utilizing a spectrophotometer at 432 nm. The quercetin concentration was computed using a calibration curve; then the EE was calculated using the following equation:

$$\text{EE}\ (\%) = \frac{C_1}{C_0} \times 100 \quad (1)$$

where C_0 and C_1 are the initial concentration of quercetin and the encapsulated amount of quercetin in nanoparticles, respectively. Furthermore, the drug loading capacity was calculated by dividing the encapsulated amount of quercetin in nanoparticles (C_1) by the total concentration of lipids (C_{lipid}) using the following equation:

$$DL\ (\%) = \frac{C_1}{C_{Lipid}} \times 100 \quad (2)$$

Evaluation of antioxidant activity

The antioxidant activity of Q-LipoDQ was evaluated using the DPPH radical scavenging method. Briefly, 2,2-diphenyl-1-picrilhydrazyl (DPPH) powder was dissolved in methanol to obtain a 50 µg/mL concentration. The sample solution, consisting of free quercetin, Q-LipoDQ LD, and Q-LipoDQ HD, was prepared with a series of concentrations of quercetin. The sample solution was then mixed with the same volume of DPPH solution, followed by incubation in dark conditions. After 30 min incubation, the absorbance of DPPH was measured; then the scavenging effect was calculated using the following equation:

$$Inhibition\ (\%) = \frac{Absorbance_{sample\ +\ DPPH}}{Absorbance_{DPPH}} \times 100 \quad (3)$$

Furthermore, the concentration needed to inhibit 50% of DPPH (IC_{50}) was then calculated. The experiment was conducted in triplicate for each sample.

Table 1. Composition of nanocarriers used in this study.

Nanocarrier type	Carrier composition			Property
	DOPE (mM)	Cholesterol (mM)	DQ (mM)	
Q-LPs	2.250	0.500	-	Non-mitochondria-targeted liposome
Q-LipoDQ LD	2.250	0.500	1.375	Hybrid nanocarrier with low density of DQ
Q-LipoDQ HD	2.250	0.500	5.500	Hybrid nanocarrier with high density of DQ

Q, Quercetin; LPs, liposomes; LD, low density; HD, high density; DQ, dequalinium; DOPE, 1,2-dioleyl-sn-glycero-3-phosphoethanolamine.

Cell culture

TM4 cells were cultured in a complete growth medium consisting of DMEM containing a high concentration of glucose and sodium pyruvate supplemented by streptomycin-penicillin and 10% (v/v) FBS under an atmospheric condition of 5% CO_2/air at 37 °C. The subculture was conducted at the confluence of 90%.

Analysis of mitochondrial accumulation level

The ability of the nanocarrier to accumulate inside the mitochondria compartment of TM4 cells was evaluated using confocal laser scanning microscopy (CLSM). We labeled the quercetin-loaded nanocarriers with coumarin 6 as the source of the fluorescent signal. Briefly, TM4 cells were cultured on a 35-mm glass base dish for 24 h to facilitate the attachment of the cells to the dish. The coumarin 6-labeled quercetin-loaded nanocarriers were transfected into the cells in a serum-free medium for 3 h. The cells underwent a washing procedure, initially utilizing PBS supplemented with 20 IU/mL heparin, followed by two additional washes conducted with a complete growth medium. MitoTracker Deep Red FM was transfected for 20 min to stain the mitochondria compartment. Then, the nucleus was stained using Hoechst 33342. The observations were carried out using CLSM (Olympus FV1200, Tokyo, Japan) equipped with a water-immersion objective lens (UPLSAPO) and a dichroic mirror (DM405/440/473/559/635). To excite the Hoechst 33342, coumarin 6, and MitoTracker Deep Red FM, cells were irradiated at optical wavelengths of 405, 473, and 635 nm, respectively. Three fluorescence detection channels were set using a filter to detect the Hoechst 33342, coumarin 6, and Mitotracker Deep Red FM. Mitochondria accumulation levels were then semi-quantitatively analyzed using ImageJ software (23) by determining Pearson's coefficient. Pearson's coefficient has a value ranging from -1 to +1. A more positive value indicates a greater correlation between two objects (24).

Evaluation of antioxidant activity in TM4 cells using H_2O_2 induction

TM4 cells were seeded on a 96-well plate. After 24 h incubation, the cells were transfected with the quercetin-loaded nanoparticles in a serum-free medium for 3 h. The medium containing nanoparticles was then replaced by a complete growth medium containing H_2O_2, and the cells were further incubated for 21 h. As a control, we prepared the cells incubated only with H_2O_2. Cell viability was determined using an MTT reagent with a 2-h incubation. The formed formazan crystals were dissolved using DMSO, and the absorbance was measured at 550 nm with a reference at 670 nm. Cell viability was calculated while the viability of the untreated cells was assumed to be 100%. The viability of cells transfected with quercetin-loaded nanocarrier was compared to the cells induced only by H_2O_2 to calculate relative viability. At least three independent experiments were conducted.

Statistical analysis

All quantitative data are presented as mean ± SD. Statistical analysis was conducted to evaluate the significance between two or more treatments. The T-test was used to analyze the difference between the two treatment groups. For the comparison of more than two groups, one-way ANOVA was employed pursued by the Student-Newman-Keuls test (SNK-test). Specifically for the evaluation of antioxidant activity in TM4 cells, two-way ANOVA followed by Tukey's multiple comparisons test was utilized.

RESULTS

Construction of mitochondria-targeted quercetin

Due to the simplicity of producing homogenous nanoparticles in a relatively short period, the LipoDQ was formed by using the hydration method. The liposomal core was built by combining DOPE and cholesterol with a molar ratio of 9:2 and a total lipid concentration of 2.75 mM, based on the previous report (25). The ratio of DQ to total lipid in the LipoDQ formulation was varied, including a low density with a 1:2 molar ratio (Q-LipoDQ LD) and a high density with a 2:1 molar ratio (Q-LipoDQ HD). Based on the hydrodynamic diameter measurement results (Fig. 2A and B), no significant differences were found between the two concentrations of DQ on the particle size

and its distribution. However, the addition of DQ into the liposomal structure led to an increase in particle size, which was probably caused by the insertion of the DQ structure into the lipid bilayer of the liposomes. The insertion of DQ into the liposome structure was also strengthened by shifting zeta potential from highly negatively charged Q-LPs (without DQ) to positively charged Q-LipoDQ (Fig. 2C). Moreover, Q-LipoDQ HD displayed more positively charged than Q-LipoDQ LD, indicating disparities in DQ densities.

Analysis of EE and drug loading capacity of quercetin

Based on the quercetin assay results, we found that approximately 62% of initial quercetin can be encapsulated into the liposomal structure. However, the amount of encapsulated quercetin slightly decreased in the presence of DQ in Q-LipoDQ LD and Q-LipoDQ HD (Fig. 3A). According to the assessment of the drug loading capacity of quercetin inside the nanocarrier, a similar trend with the result of EE was found in drug loading capacity, in which the Q-LPs showed relatively higher drug loading capacity compared to Q-LipoDQ (Fig. 3B). A reduction in EE might be due to the lipid bilayer membrane stretching. This occurred due to electrostatic interactions between the positively charged DQ and the negatively charged lipid head groups. This interaction causes the bilayer membrane to expand, owing to the repulsive force created by the two delocalized positive charges of DQ (26).

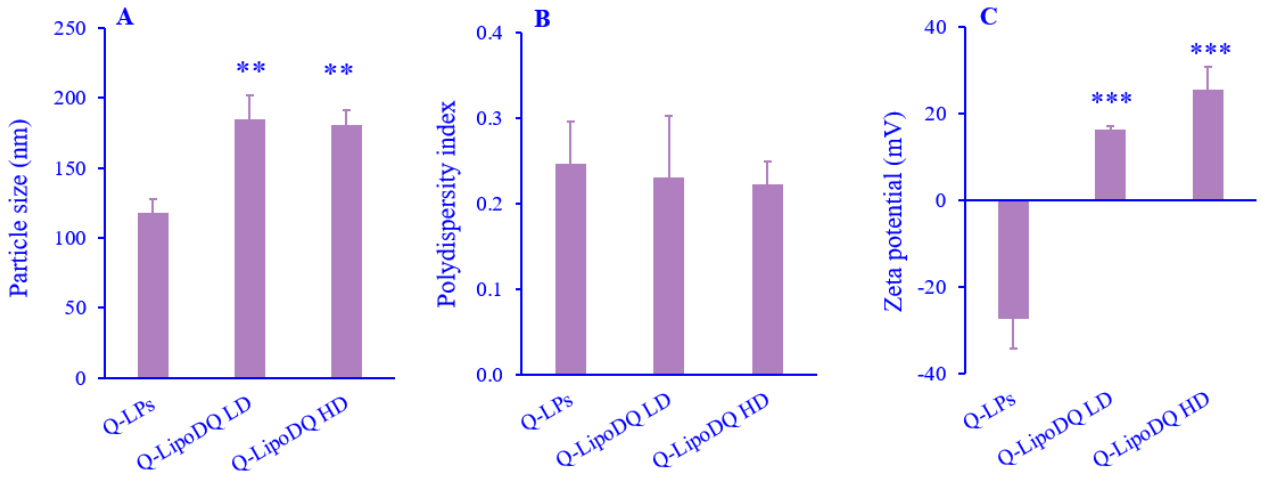

Fig. 2. Particle characteristics of quercetin encapsulated in nanocarrier systems. (A) Hydrodynamic diameter of the particles (n = 5); (B) polydispersity index (n = 5), and (C) zeta potential (n = 3). Values represent mean ± SD. $^{**}P < 0.01$ and $^{***}P < 0.001$ indicate significant differences in comparison with the Q-LPs group. Q, Quercetin; LPs, liposomes; LD, low density; HD, high density; DQ, dequalinium.

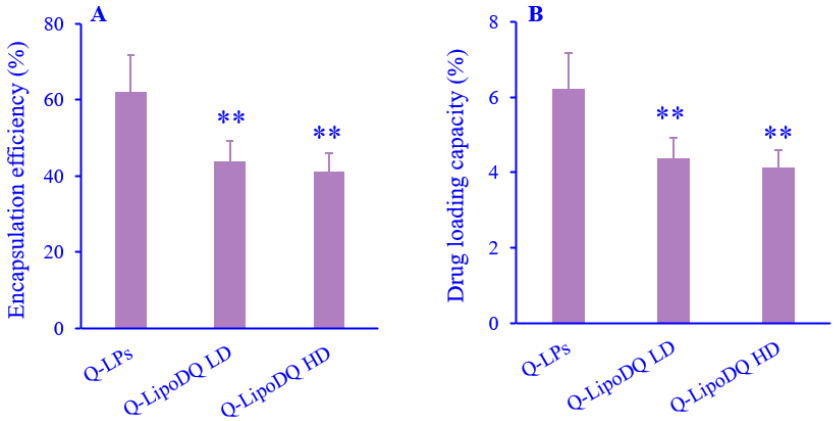

Fig. 3. (A) Encapsulation efficiency and (B) drug loading capacity of quercetin inside the nanocarrier system. Values represent mean ± SD, n = 5. $^{**}P < 0.01$ Indicates significant differences in comparison with the Q-LPs group. Q, Quercetin; LPs, liposomes; LD, low density; HD, high density; DQ, dequalinium.

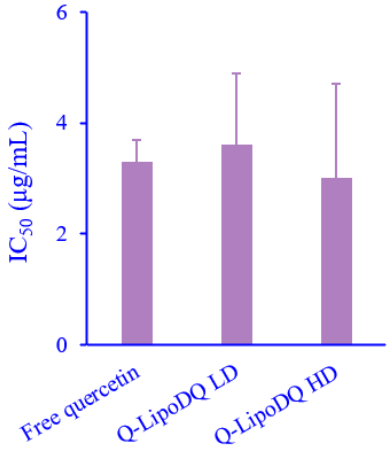

Fig. 4. The IC_{50} values of free quercetin in methanolic solution, Q-LipoDQ LD, and Q-LipoDQ HD using the DPPH radical scavenging method. Values represent mean ± SD, n = 3. Q, Quercetin; LPs, liposomes; LD, low density; HD, high density; DQ, dequalinium; DPPH, 2,2-diphenyl-1-picrilhydrazyl.

Validation of the antioxidant potential of quercetin

To anticipate the reduction of the antioxidant potential of quercetin during the encapsulation process into nanocarrier, the antioxidant activity assay using the DPPH radical scavenging method was performed. In this study, we compared the antioxidant activity of free quercetin molecules in a methanolic solution with Q-LipoDQ LD and Q-LipoDQ HD. The IC_{50} values of free quercetin molecules, Q-LipoDQ LD, and Q-LipoDQ HD were not statistically different (Fig. 4). This result indicates that the encapsulation of quercetin into LipoDQ structure did not affect its free radical scavenging capacity.

Intracellular trafficking analysis

The ability of LipoDQ to deliver quercetin into the mitochondrial compartment of TM4 cells was determined using confocal laser scanning microscopy (CLSM). In this evaluation, coumarin 6 was added to label all quercetin-loaded nanocarriers. Furthermore, the mitochondria and nucleus of TM4 cells were stained using MitoTracker Deep Red FM and Hoechst 33342, respectively. Qualitatively, the green fluorescence signal of Q-LPs was separated from the red fluorescence signal of MitoTracker Deep Red FM (Fig. 5A), indicating low mitochondrial accumulation. In contrast, a robust yellow signal was obtained on the cells transfected by Q-LipoDQ, regardless of the concentration of DQ. The yellow signals appeared due to overlapping the green and red fluorescence signals of Q-LipoDQ and mitochondria, respectively. The observed yellow signals indicate the accumulation of Q-LipoDQ inside the mitochondrial compartment of TM4 cells. Moreover, all tested nanocarriers displayed negligible accumulation in the nucleus. To further substantiate the level of mitochondrial accumulation the correlation between the fluorescence signals emitted from coumarin 6 and MitoTracker Deep Red FM was assessed using Pearson's coefficient. Pearson's coefficient was calculated using ImageJ software from several CLSM images. As shown in Fig. 5B, Q-LPs exhibited the lowest Pearson's coefficient value relative to Q-LipoDQ, indicating a low mitochondrial accumulation level. Interestingly, the difference in DQ density did not significantly affect the mitochondrial accumulation level of Q-LipoDQ.

In vitro antioxidant activity in TM4 cells under H_2O_2 induction

To investigate the protective effects of quercetin-loaded nanocarriers on the oxidative stress in TM4 cells, the H_2O_2-induced cell viability was assessed. In the preliminary study, TM4 cells were transfected with various concentrations of H_2O_2, and cell viability was measured using MTT assay. TM4 cell viability was H_2O_2 concentration-dependent (data not shown). H_2O_2 at 1 mM caused approximately 50% cell death; therefore, this concentration was utilized in the subsequent experimental procedures. Furthermore, the quercetin-loaded nanocarriers were transfected into TM4 cells before the induction of oxidative stress using H_2O_2, and the cell viability was measured using MTT assay. Figure 6 displays the relative viability of TM4 cells upon treatment with Q-LPs, Q-LipoDQ LD, and Q-LipoDQ HD at different concentrations of quercetin ranging from 0.01 µM to 0.1 µM, compared to cells induced only by H_2O_2.

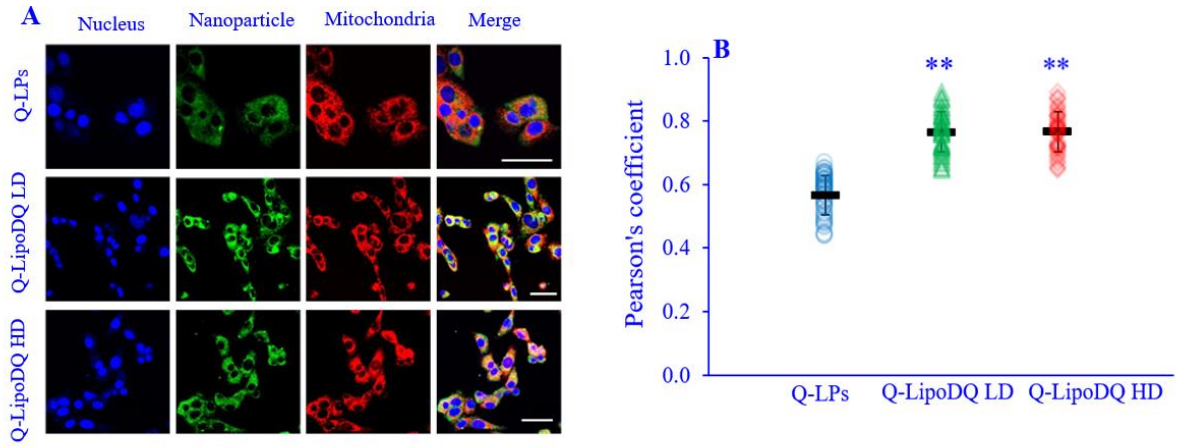

Fig. 5. Intracellular trafficking analysis of Q-LPs, Q-LipoDQ LD, and Q-LipoDQ HD in TM4 cells. (A) Representative CLSM images of TM4 cells treated with several quercetin-loaded nanocarriers. The nanoparticle was labeled by coumarin 6, while mitochondria and nucleus were stained using MitoTracker Deep Red FM and Hoechst 33342, respectively. Scale bars: 50 µm. (B) Semi-quantitative measurement of mitochondrial colocalization level using Pearson's coefficient from several randomly selected CLSM images. Error bars indicate SD, n = 50, $^{**}P < 0.01$ Indicates significant differences in comparison with the Q-LPs group. Q, Quercetin; LPs, liposomes; LD, low density; HD, high density; DQ, dequalinium.

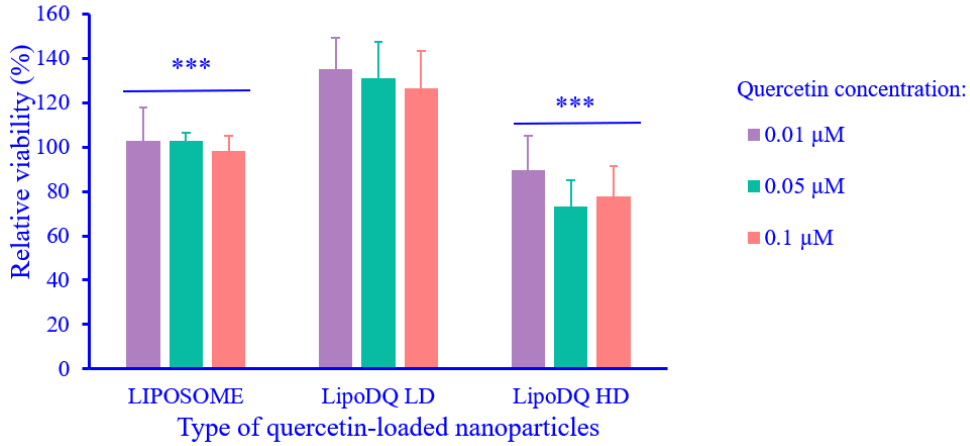

Fig. 6. Viability of TM4 cells pre-treated with various concentrations of quercetin delivered by Q-LPs, Q-LipoDQ LD, and Q-LipoDQ HD during H_2O_2 induction. Values represent mean ± SD, n = 4. $^{***}P < 0.001$ indicates significant differences compared to the LipoDQ LD group at the respective concentration of quercetin. Q, Quercetin; LPs, liposomes; LD, low density; HD, high density; DQ, dequalinium.

The results indicated that the type of nanoparticles used to deliver quercetin is the primary factor influencing the relative viability of TM4 cells. Moreover, treatment with Q-LPs and Q-LipoDQ HD did not increase the relative viability in all quercetin concentrations tested. Additionally, increasing the concentration of quercetin in Q-LipoDQ HD led to a further decrease in relative viability. On the other hand, the cells pre-treated with Q-LipoDQ LD exhibited significantly higher relative viability at all tested quercetin concentrations, indicating the protective effect against oxidative stress ($P_{\text{Type of nanoparticles}} < 0.001$, $P_{\text{Quercetin concentrations}} = 0.275$, $P_{\text{Interaction}} = 0.784$).

DISCUSSION

In this research, we utilized quercetin as a model antioxidant to be delivered into the mitochondria of Sertoli cells. Quercetin is a polyphenolic flavonoid bioactive molecule widely found in several plants, including tea, onions, apples, Asiatic pennywort, leaf cabbage, and many more (27). Quercetin has numerous pharmacological benefits, including antioxidant, anti-inflammatory, anti-diabetic, antihypertensive, and anti-hypercholesterolemic activities (28). The antioxidant activity of quercetin mainly involves enhancing the endogenous antioxidant capacity and

neutralizing ROS (29). Despite the beneficial activities of quercetin, it retains several limitations regarding solubility, stability, and low bioavailability, making the formulation process of this compound challenging. Furthermore, the efficacy of quercetin is limited due to its non-specific accumulation inside the cells, which hinders its potential benefits. To overcome these challenges, we developed a hybrid nanoplatform to deliver quercetin into the mitochondria of cells.

The liposomal system created using DOPE and cholesterol was combined with a mitochondriotropic molecule of DQ to form a hybrid nanoplatform. The nanoplatform was designed to deliver quercetin specifically into the mitochondria compartment of Sertoli cells. DOPE was selected as the main lipid due to the pH-sensitive fusogenic activity that may help the endosomal escape process (30). Furthermore, the presence of cholesterol as a helper lipid could improve the rigidity and stability of the liposomal structure (31,32), which may protect quercetin from degradation and premature drug release. On the other hand, DQ consists of two aminoquinaldinium rings connected by a hydrophobic hydrocarbon chain. The insertion of the DQ molecule into the liposomal structure is possibly achieved through the hydrophobic interaction between the hydrocarbon chain of DQ and the lipid bilayer of the liposome (33). Moreover, the cationic aminoquinaldinium rings will be oriented on the surface of the liposome, resulting in a positively charged particle, as indicated by zeta potential analysis.

We conducted a study to determine the concentration of quercetin encapsulated in nanocarriers. The study was performed directly by analyzing the amount of quercetin encapsulated inside the nanocarrier system. First, the quercetin-loaded nanocarrier was purified from non-encapsulated quercetin using centrifugation at 16,000 rpm, 4 °C for 10 min. This method was selected due to the poor water solubility of quercetin; thus, the non-encapsulated quercetin can be easily sedimented using a centrifugation process. On the other hand, the 16,000-rpm centrifugation speed is not sufficiently strong to sediment the nanocarrier (34). The concentration of quercetin inside the nanoparticle was determined by complexing the quercetin with $AlCl_3$ in a sodium acetate solution. This complexation reaction produced a stable complex with a maximum absorbance at 415-450 nm (22). Despite a decrease in the EE of quercetin in the LipoDQ system, the EE of quercetin in the Q-LipoDQ structure remains comparable to that of previous quercetin-loaded deformable liposomes composed of soybean phosphatidylcholine and cholesterol in a 4:1 weight ratio (35).

The encapsulation process of a drug into a nanocarrier system involves several steps that may affect the stability and physicochemical properties of the encapsulated drug, thereby affecting its pharmacological activities. The DPPH radical scavenging analysis was performed to evaluate the antioxidant activity of quercetin before and after the encapsulation process. DPPH is a stable free radical molecule with a dark violet color and a maximum absorbance in ethanol solution around 520 nm (36). The reaction between DPPH and hydrogen donor molecules (antioxidants) reduces DPPH to a hydrazine molecule. This reduction is characterized by the decolorization process, indicated by a decrease in solution absorbance. The antioxidant activity of all Q-LipoDQ was equivalent to free quercetin, with the IC_{50} values ranging from 3.0 to 3.6 μM. This antioxidant activity can be classified as a notably robust antioxidant, which can potentially be utilized to mitigate the oxidative stress in Sertoli cells.

After observing the high potential antioxidant activity of Q-LipoDQ, we investigated the intracellular trafficking of Q-LipoDQ in Sertoli cells. As part of this study, we employed TM4 cells to represent Sertoli cells. TM4 cells are an established epithelial cell line isolated from the testis of immature BALB/c mice. This cell line was identified to have Sertoli cell properties since it displayed a growth response during the induction with follicle-stimulating hormone but not in the presence of the luteinizing hormone (LH) (37). TM4 cells are widely used to study male reproductive function and fertility (38,39) due to their simple handling and culture relative to Sertoli cell primary cultures (40). To conduct the intracellular trafficking analysis, we first stained all quercetin-loaded nanocarriers using coumarin 6 as a fluorescent probe. Coumarin 6 is a coumarin derivative that can fluoresce at

512 nm upon excitation at 460 nm (41). Due to its hydrophobic characteristics, coumarin 6 is highly accumulated inside the hydrophobic lipid bilayer of liposomes (42). As a result, the Q-LPs were marginally accumulated inside the mitochondrial compartment of TM4 cells. Q-LipoDQ, regardless of the DQ concentration, was, however, strongly accumulated inside the mitochondria of TM4 cells. This result confirms the crucial role of DQ moieties on the surface of liposomes in determining their ability to accumulate in mitochondria. Furthermore, a DQ concentration-independent profile was obtained by transporting quercetin selectively into the mitochondrial compartment of TM4 cells.

Encouraged by the potential antioxidant activity of Q-LipoDQ evaluated by the DPPH radical scavenging method, as well as the capacity of LipoDQ in delivering quercetin into the mitochondrial compartment of TM4 cells, we then proceeded to evaluate the protective effect of Q-LipoDQ in TM4 cells under the H_2O_2 induction. The transfection of an excessive amount of H_2O_2 induces oxidative stress, leading to cell death (43). Additionally, H_2O_2 generates mitochondrial dysfunction and induces apoptosis by lowering the mitochondrial membrane potential, thus triggering the release of cytochrome c (44). The *in vitro* antioxidant activity results manifested that Q-LipoDQ LD provided a significantly higher level of protection than Q-LPs and Q-LipoDQ HD. Interestingly, while Q-LipoDQ HD has similar DPPH scavenging activity and mitochondrial accumulation levels as Q-LipoDQ LD, it failed to protect TM4 cells from oxidative stress. Moreover, the higher concentration of quercetin inside the Q-LipoDQ HD provoked more massive cell death. These results can be explained due to the high density of DQ, which could aggravate mitochondrial function by altering the redox balance, which was concentration-dependent (21). On the other hand, Q-LPs were ineffective in protecting TM4 cells from oxidative stress owing to their non-specific cellular accumulation.

The results from the antioxidant activity in TM4 cells, along with analysis of intracellular trafficking, suggests that Q-LipoDQ LD can rescue TM4 cells from the harmful effects of H_2O_2-induced oxidative stress and mitochondrial dysfunction. Moreover, these results also validate the importance of controlling ROS levels in the mitochondria of TM4 cells, which can be achieved by delivering exogenous antioxidants specifically to the mitochondrial compartment.

CONCLUSION

A mitochondria-targeted hybrid nano-platform was successfully developed to deliver quercetin, namely Q-LipoDQ, which was built by incorporating DQ into a liposomal structure. The encapsulation of quercetin into LipoDQ exhibited a negligible change in the antioxidant capacity of quercetin, indicated by the similar IC_{50} value of the free radical scavenging activity. The Q-LipoDQ was also found to have dominant mitochondrial accumulation, regardless of the DQ concentration. However, only Q-LipoDQ LD could rescue the negative effect of oxidative stress in TM4 cells, while Q-LipoDQ HD disrupted mitochondrial function, leading to a significant decrease in cell viability. Finally, the findings explained in this research verify the potential of LipoDQ LD as a mitochondria-targeted hybrid nanoplatforms that can safely be used for delivering exogenous antioxidants specific to the mitochondrial compartment of the cells. Furthermore, this research also revealed the importance of mitochondrial delivery of antioxidants to relieve the harmful effect of oxidative stress in Sertoli cells.

Acknowledgments

This work was financially supported by Riset Pengembangan Kapasitas Dosen Muda ITB 2021 (Grant No. 147/IT1.B07.1/ TA.00/2021) from the Institute for Research and Community Services of Institut Teknologi Bandung. We are also grateful to Olympus-ITB Bio Imaging Center for providing us with a confocal laser scanning microscope.

Satrialdi is the recipient of a research grant namely Riset Pengembangan Kapasitas Dosen Muda ITB 2021 from the Institute for Research and Community Services of Institut Teknologi Bandung.

Conflict of interest statement

The authors declared no conflict of interest in this study.

Authors' contributions

Satrialdi contributed to conceptualization, funding acquisition, methodology, supervision, visualization, and writing of the original draft, review, and editing. C. Pratiwi and R. Novia Khaeranny contributed to the data curation, formal analysis, and investigation. D. Mudhakir contributed to conceptualization, funding acquisition, supervision, writing, review, and editing.

REFERENCES

1. Tremellen K. Oxidative stress and male infertility-a clinical perspective. Hum Reprod Update. 2008;14(3):243-258. DOI: 10.1093/humupd/dmn004.
2. Andersen JM, Rønning PO, Herning H, Bekken SD, Haugen TB, Witczak O. Fatty acid composition of spermatozoa is associated with BMI and with semen quality. Andrology. 2016;4(5):857-865. DOI: 10.1111/andr.12227.
3. Agarwal A, Prabakaran SA. Mechanism, measurement, and prevention of oxidative stress in male reproductive physiology. Indian J Exp Biol. 2005;43(11):963-974. PMID: 16315393.
4. Nowak JZ. Oxidative stress, polyunsaturated fatty acidsderived oxidation products and bisretinoids as potential inducers of CNS diseases: focus on age-related macular degeneration. Pharmacol Reports. 2013;65(2):288-304. DOI: 10.1016/S1734-1140(13)71005-3.
5. Sabeti P, Pourmasumi S, Rahiminia T, Akyash F, Talebi AR. Etiologies of sperm oxidative stress. Int J Reprod Biomed. 2016;14(4):231-240. PMID: 27351024.
6. Kowalczyk A. The role of the natural antioxidant mechanism in sperm cells. Reprod Sci. 2022;29(5):1387-1394. DOI: 10.1007/s43032-021-00795-w.
7. Snezhkina AV, Kudryavtseva AV, Kardymon OL, Savvateeva MV, Melnikova NV, Krasnov GS, *et al*. ROS generation and antioxidant defense systems in normal and malignant cells. Oxid Med Cell Longev. 2019;2019:1-17. DOI: 10.1155/2019/6175804.
8. Finkel T. Signal transduction by reactive oxygen species. J Cell Biol. 2011;194(1):7-15. DOI: 10.1083/jcb.201102095.
9. Guerriero G, Trocchia S, Abdel-Gawad FK, Ciarcia G. Roles of reactive oxygen species in the spermatogenesis regulation. Front Endocrinol (Lausanne). 2014;5(56):1-4. DOI: 10.3389/fendo.2014.00056.
10. Alahmar A. Role of oxidative stress in male infertility: an updated review. J Hum Reprod Sci. 2019;12(1):4-18. DOI: 10.4103/jhrs.JHRS_150_18.
11. Vertika S, Singh KK, Rajender S. Mitochondria, spermatogenesis, and male infertility - an update. Mitochondrion. 2020;54:26-40. DOI: 10.1016/j.mito.2020.06.003.
12. Varuzhanyan G, Rojansky R, Sweredoski MJ, Graham RLJ, Hess S, Ladinsky MS, *et al*. Mitochondrial fusion is required for spermatogonial differentiation and meiosis. Elife. 2019;8:1-27. DOI: 10.7554/eLife.51601.
13. Yamada Y, Satrialdi, Hibino M, Sasaki D, Abe J, Harashima H. Power of mitochondrial drug delivery systems to produce innovative nanomedicines. Adv Drug Deliv Rev. 2020;154-155:187-209. DOI: 10.1016/j.addr.2020.09.010.
14. Rossman MJ, Santos-Parker JR, Steward CAC, Bispham NZ, Cuevas LM, Rosenberg HL, *et al*. Chronic supplementation with a mitochondrial antioxidant (MitoQ) improves vascular function in healthy older adults. Hypertension. 2018;71(6):1056-1063. DOI: 10.1161/HYPERTENSIONAHA.117.10787.
15. Zupančič Š, Kocbek P, Zariwala MG, Renshaw D, Gul MO, Elsaid Z, *et al*. Design and development of novel mitochondrial targeted nanocarriers, DQAsomes for curcumin inhalation. Mol Pharm. 2014;11(7):2334-2345. DOI: 10.1021/mp500003q.
16. Wu J, Zhang M, Hao S, Jia M, Ji M, Qiu L, *et al*. Mitochondria-targeted peptide reverses mitochondrial dysfunction and cognitive deficits in sepsis-associated encephalopathy. Mol Neurobiol. 2015;52(1):783-791. DOI: 10.1007/s12035-014-8918-z.
17. Kubota F, Satrialdi, Takano Y, Maeki M, Tokeshi M, Harashima H, *et al*. Fine-tuning the encapsulation of a photosensitizer in nanoparticles reveals the relationship between internal structure and phototherapeutic effects. J Biophotonics. 2023;16(3):1-11. DOI: 10.1002/jbio.202200119.
18. Trnka J, Elkalaf M, Anděl M. Lipophilic triphenylphosphonium cations inhibit mitochondrial electron transport chain and induce mitochondrial proton leak. PLoS One. 2015;10(4):e0121837,1-14. DOI: 10.1371/journal.pone.0121837.
19. Weissig V, Lasch J, Erdos G, Meyer HW, Rowe TC, Hughes J. DQAsomes: a novel potential drug and gene delivery system made from *Dequalinium*. Pharm Res. 1998;15(2):334-337. DOI: 10.1023/a:1011991307631.
20. Weissig V, Lizano C, Torchilin VP. Selective DNA release from DQAsome/DNA complexes at mitochondria-like membranes. Drug Deliv. 2000;7(1):1-5. DOI: 10.1080/107175400266722.
21. García-Pérez AI, Galeano E, Nieto E, Sancho P. Dequalinium induces human leukemia cell death by affecting the redox balance. Leuk Res. 2011;35(10):1395-1401. DOI: 10.1016/j.leukres.2011.03.012.
22. Chang CC, Yang MH, Wen HM, Chern JC. Estimation of total flavonoid content in propolis by

two complementary colometric methods. J Food Drug Anal. 2020;10(3):178-182.
DOI: 10.38212/2224-6614.2748.
23. Schindelin J, Arganda-Carreras I, Frise E, Kaynig V, Longair M, Pietzsch T, *et al*. Fiji: an open-source platform for biological-image analysis. Nat Methods. 2012;9(7):1-15.
DOI: 10.1038/nmeth.2019.
24. Adler J, Parmryd I. Quantifying colocalization by correlation: the Pearson correlation coefficient is superior to the Mander's overlap coefficient. Cytom Part A. 2010;77(8):733742.
DOI: 10.1002/cyto.a.20896.
25. Satrialdi, Takano Y, Hirata E, Ushijima N, Harashima H, Yamada Y. An effective *in vivo* mitochondria-targeting nanocarrier combined with a π-extended porphyrin-type photosensitizer. Nanoscale Adv. 2021;3(20):5919-5927.
DOI: 10.1039/D1NA00427A.
26. Sauvage F, Legrand FX, Roux M, Rajkovic I, Weiss TM, Varga Z, *et al*. Interaction of dequalinium chloride with phosphatidylcholine bilayers: a biophysical study with consequences on the development of lipid-based mitochondrial nanomedicines. J Colloid Interface Sci. 2019;537:704-715.
DOI: 10.1016/j.jcis.2018.11.059.
27. Anand David A, Arulmoli R, Parasuraman S. Overviews of biological importance of quercetin: a bioactive flavonoid. Pharmacogn Rev. 2016;10(20):84-89.
DOI: 10.4103/0973-7847.194044.
28. Batiha GES, Beshbishy AM, Ikram M, Mulla ZS, El-Hack MEA, Taha AE, *et al*. The Pharmacological activity, biochemical properties, and pharmacokinetics of the major natural polyphenolic flavonoid: quercetin. Foods. 2020;9(3):374,1-16.
DOI: 10.3390/foods9030374.
29. Xu D, Hu MJ, Wang YQ, Cui YL. Antioxidant activities of quercetin and its complexes for medicinal application. Molecules. 2019;24(6):1123,1-15.
DOI: 10.3390/molecules24061123.
30. Cardarelli F, Pozzi D, Bifone A, Marchini C, Caracciolo G. Cholesterol-dependent macropinocytosis and endosomal escape control the transfection efficiency of lipoplexes in CHO living cells. Mol Pharm. 2012;9(2):334-340.
DOI: 10.1021/mp200374e.
31. Liu DZ, Chen WY, Tasi LM, Yang SP. Microcalorimetric and shear studies on the effects of cholesterol on the physical stability of lipid vesicles. Colloids Surfaces A Physicochem Eng Asp. 2000;172(1-3):57-67.
DOI: 10.1016/S0927-7757(00)00560-4.
32. Briuglia ML, Rotella C, McFarlane A, Lamprou DA. Influence of cholesterol on liposome stability and on *in vitro* drug release. Drug Deliv Transl Res. 2015;5(3):231-242.
DOI: 10.1007/s13346-015-0220-8.
33. Bae Y, Jung MK, Song SJ, Green ES, Lee S, Park HS, *et al*. Functional nanosome for enhanced mitochondria-targeted gene delivery and expression. Mitochondrion. 2017;37:27-40.
DOI: 10.1016/j.mito.2017.06.005.
34. Lin M, Qi XR. Purification method of drug-loaded liposome. In: Wan-Liang L, Xian-Rong Q. Liposome-based drug delivery systems. 2019. pp. 1-11.
DOI: 10.1007/978-3-662-49231-4_24-1.
35. Liu D, Hu H, Lin Z, Chen D, Zhu Y, Hou S, *et al*. Quercetin deformable liposome: preparation and efficacy against ultraviolet B induced skin damages *in vitro* and *in vivo*. J Photochem Photobiol B. 2013;127:8-17.
DOI: 10.1016/j.jphotobiol.2013.07.014.
36. Kedare SB, Singh RP. Genesis and development of DPPH method of antioxidant assay. J Food Sci Technol. 2011;48(4):412-422.
DOI: 10.1007/s13197-011-0251-1.
37. Matfier JP. Establishment and characterization of two distinct mouse testicular epithelial cell line. Biol Reprod. 1980;23(1):243-252.
DOI: 10.1095/biolreprod23.1.243.
38. Wu L, Dong H, Zhao J, Wang Y, Yang Q, Jia C, *et al*. Diosgenin stimulates rat TM4 cell proliferation through activating plasma membrane translocation and transcriptional activity of estrogen receptors1. Biol Reprod. 2015;92(1):24,1-10.
DOI: 10.1095/biolreprod.114.124206.
39. Ni Z, Sun W, Li R, Yang M, Zhang F, Chang X, *et al*. Fluorochloridone induces autophagy in TM4 Sertoli cells: involvement of ROS-mediated AKT-mTOR signaling pathway. Reprod Biol Endocrinol. 2021;19(1):64,1-13.
DOI: 10.1186/s12958-021-00739-8.
40. Luo Y, Mohsin A, Xu C, Wang Q, Hang H, Zhuang Y, *et al*. Co-culture with TM4 cells enhances the proliferation and migration of rat adipose-derived mesenchymal stem cells with high stemness. Cytotechnology. 2018;70(5):1409-1422.
DOI: 10.1007/s10616-018-0235-3.
41. Kristoffersen AS, Erga SR, Hamre B, Frette Ø. Testing fluorescence lifetime standards using two-photon excitation and time-domain instrumentation: rhodamine B, coumarin 6 and lucifer yellow. J Fluoresc. 2014;24(4):1015-1024.
DOI: 10.1007/s10895-014-1368-1.
42. Zhang X, Lin C, Lu A, Lin G, Chen H, Liu Q, *et al*. Liposomes equipped with cell penetrating peptide BR2 enhances chemotherapeutic effects of cantharidin against hepatocellular carcinoma. Drug Deliv. 2017;24(1):986-998.
DOI: 10.1080/10717544.2017.1340361.
43. Gokce EH, Korkmaz E, Tuncay-Tanriverdi, Dellera E, Sandri G, Bonferoni MC, *et al*. A comparative evaluation of coenzyme Q10-loaded liposomes and solid lipid nanoparticles as dermal antioxidant carriers. Int J Nanomedicine. 2012;7:5109-5117.
DOI: 10.2147/IJN.S34921.
44. Chen L, Wu X, Shen T, Wang X, Wang S, Wang J, *et al*. Protective effects of ethyl gallate on H_2O_2-induced mitochondrial dysfunction in PC12 cells. Metab Brain Dis. 2019;34(2):545-555.
DOI: 10.1007/s11011-019-0382-z.